LASER INTERFEROMETER GRAVITATIONAL WAVE OBSERVATORY
- LIGO -
CALIFORNIA INSTITUTE OF TECHNOLOGY
MASSACHUSETTS INSTITUTE OF TECHNOLOGY

Technical Note	**LIGO-T11XXXXX–vX**	2014/10/31

Orthogonal Actuators for Xarm Auxiliary Laser and Orthogonal Sensors for the Input Mode Cleaner

Andres Medina
Mentors: Dr. Nicolas Smith-Lefebre and Dr. Gabriele Vajente
The Fu Foundation of Engineering and Applied Science, Columbia University, and California Institute of Technology

California Institute of Technology
LIGO Project, MS 18-34
Pasadena, CA 91125
Phone (626) 395-2129
Fax (626) 304-9834
E-mail: info@ligo.caltech.edu

Massachusetts Institute of Technology
LIGO Project, Room NW22-295
Cambridge, MA 02139
Phone (617) 253-4824
Fax (617) 253-7014
E-mail: info@ligo.mit.edu

LIGO Hanford Observatory
Route 10, Mile Marker 2
Richland, WA 99352
Phone (509) 372-8106
Fax (509) 372-8137
E-mail: info@ligo.caltech.edu

LIGO Livingston Observatory
19100 LIGO Lane
Livingston, LA 70754
Phone (225) 686-3100
Fax (225) 686-7189
E-mail: info@ligo.caltech.edu

http://www.ligo.caltech.edu/

Abstract

The sensitivity of the 40 meter prototype interferometer detector depends on the alignment of the optical elements with respect to the incoming laser. Because the interferometer operates in the dark fringe, it is curtail that the arms are well aligned in order for acquiring and maintaining resonance. Any misalignment decreases the signal noise ratio by introducing inside the cavity spatial higher order TEM modes, and therefore introducing noise inside the cavity. In order to correct for any misalignment inside a cavity, orthogonal sensor and actuators are used to control the different degrees of freedom. The aims of this paper are to develop an optical setup that comprises orthogonal actuators for the current x-arm auxiliary laser and develop an optical setup for the Input Mode Cleaner, which also utilizes orthogonal sensors. We will design the optical setup in the given space that is available on the describe table dimension and characterize the systems orthogonally.

1 Introduction

In his theory of general relativity, Albert Einstein predicted the existence of gravitational waves (GWs). Gravitational waves are ripples in space-time curvature that propagate at the speed of light away from their source in all directions. GWs are produced from sources such as black holes and supernovae explosions. They are predicted to be transverse and quadruple in nature[2]. GWs have two polarizations that interact weakly with matter by exerting a strain on it[1]. For instance, if a ring of free masses is located in the x-y plane and a gravitational wave is propagating in the z-axis, the gravitational wave would deform the ring of free masses into an ellipse as shown in Figure 1. As it is illustrated in Figure 1, depending on the polarization, gravitational wave will interact different with matter. The length by which the ring of free masses would deform is given by $\Delta L = hL$, where L represent the radius of the ring of free masses.

In order to detect gravitational waves, two suitable GWs detectors of 4 km long with Fabry-Perot cavity arms were built: one in Hanford, WA and the other one in Livingston, LA. Since the interferometer operates on the dark fringe, it would be able to detect any change in the length in any of the arm. For instance, when gravitational waves emitted from sources, such as the merger of neutral stars or a black holes, passed through the detector, it would stretch one arm while shrinking the other arm as shown in the example of the ring of free masses in Figure 1. However, the merger of two neutron stars that are located at the other end of our galaxy would produce a gravitational wave strain of order $h \simeq 10^{-19}$[2]. In order to detect this signal, this would require the detector to have a strong signal to noise ratio. Therefore, the interferometer must be well aligned at all times. Any misalignment would introduce higher order TEM modes and would reduce the signal to noise ratio because of reduction of the power circulating inside the cavity. Misalignment can easily be corrected by having orthogonal sensors and actuators that detect any misalignment and correct for it. In this paper, I will characterize the current auxiliary laser actuators, and I will design a new optical setup that comprise orthogonality between the actuators. Then, I would characterize the current input mode cleaner sensor orthogonality and lastly design a system that incorporate orthogonality between the wavefront sensors.

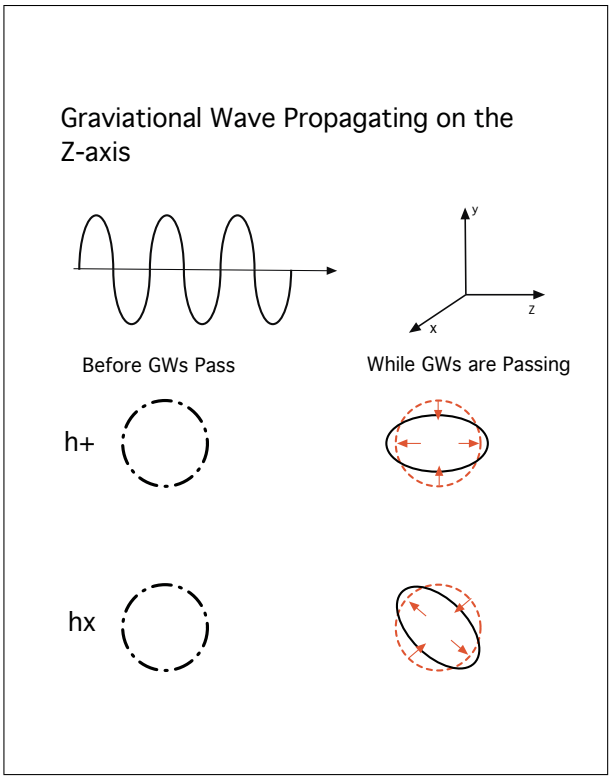

Figure 1: The effect that the two polarizations of the gravitational wave would have on a ring of free test masses.

2 Gaussian Beam and the Phase Space Representation for the Alignment of Optical System

2.1 Gaussian Beam and Its Properties

Before we take a look into the current auxiliary laser alignment issues, let's us familiarize ourself with some basis concepts.The most interesting solution of the Paraxial Helmholtz Equation is the Gaussian beam [4]. The Paraxial Helmholtz equation is given by $\nabla^2{}_T A - 2jk\frac{\partial A}{\partial z} = 0$. The equation of a Gaussian beam is given by $U(\boldsymbol{r}) = A_0 \frac{w_0}{w(z)} exp[-\frac{\rho^2}{w^2(z)}] exp[-jkz - jk\frac{\rho^2}{2R(z)} + j\varphi(z)]$, where w_0 is the beam waist size, R is the radius of curvature of the beam, $\rho = x^2 + y^2$, and $\varphi(z)$ is a phase shift that the gaussian beam acquires as it propagates

through space. The beam parameters are:

$$w(z) = w_0\sqrt{1+\left(\frac{z}{z_R}\right)^2} \tag{1}$$

$$R(z) = z\left[1+\left(\frac{z_R}{z}\right)^2\right] \tag{2}$$

$$\varphi(z) = tan^{-1}\left(\frac{z}{z_R}\right) \tag{3}$$

$$w_0 = \sqrt{\frac{\lambda z_R}{\pi}} \tag{4}$$

$$z_R = \frac{\pi {w_0}^2}{\lambda} \qquad \text{Rayleigh range} \tag{5}$$

As a gaussian beam propagates through space or through an optical medium it acquires a phase shift that differs from a plane wave of the same optical frequency. In physical terms, the phase velocity and the spacing between the phase fronts are slightly larger than an ideal plane wave [5]. This phase shift that a gaussian beam acquires is called the Gouy phase, and it ranges between -90 at $z = -\infty$ and 90 at $z = \infty$ as shown in Figure 2. Later, we will discuss in more details about the significance of the Gouy phase.

The gaussian beam solution presented above it is the lowest-order solution. There are actually an infinite family of higher order Hermite-gaussian beams. The higher order Hermite-Gaussian is given by the following expression:

$$U_{n,m}(x,y,z) = A_{n,m}\left[\frac{w_0}{w(z)}\right]H_n\left[\frac{\sqrt{2}x}{w(z)}\right]H_m\left[\frac{\sqrt{2}y}{w(z)}\right] \times exp\left[-jkz - jk\frac{x^2+y^2}{2R(z)} + j(n+m+1)\varphi(z)\right] \tag{6}$$

where H_n and H_m represent the Hermite polynomial of order n and m respectively. In Figure 3, it shows a Hermite-Gaussian beam intensity profile in which the fundamental TEM_{00} mode is the lowest order gaussian mode. We can observe that the Gouy phase between the TEM_{00} gaussian beam is just φ at any plane z, while the higher order TEM_{nm} Hermite-gaussian beam has a Gouy phase of $(n+m+1)\varphi$. This will become significance when looking at misaligning. It has been shown by Anderson[9] that misalignment is just a superposition between the TEM_{00} mode and TEM_{01}. If we take the normalized lowest two order Hermite-Gaussian beam, and we introduce a small beam displacement a_x in the TEM_{00} Hermite-Gaussian beam, we get $\psi(x) \simeq A\left(\frac{2}{\pi {x_o}^2}\right)^{\frac{1}{4}}\left(1+2a_x\frac{x}{{x_o}^2}\right)exp\left[-\left(\frac{x}{x_o}\right)^2\right]$[9]. Therefore, misalignment is a superposition between the TEM_{00} mode and higher Hermite-gaussian modes.

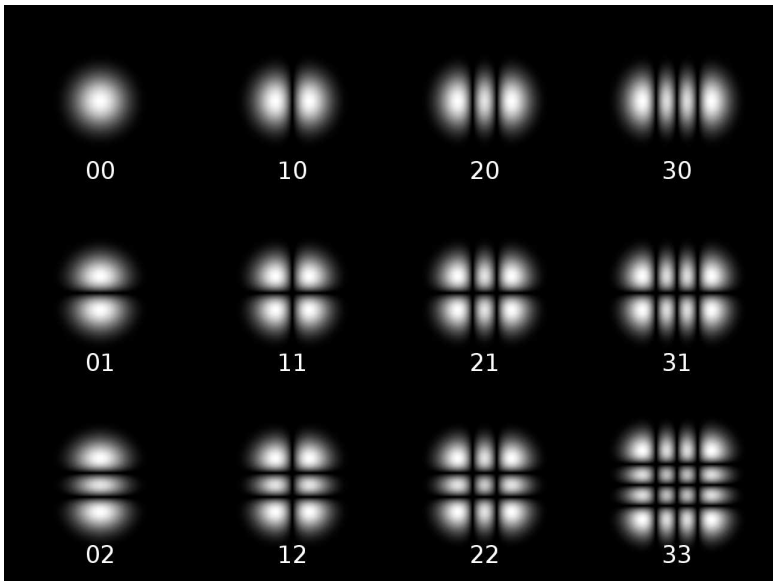

Figure 3: Intensity distribution from lowest to higher order Hermite-gaussian[7]. The TEM_{nm} order are indicated in each case.

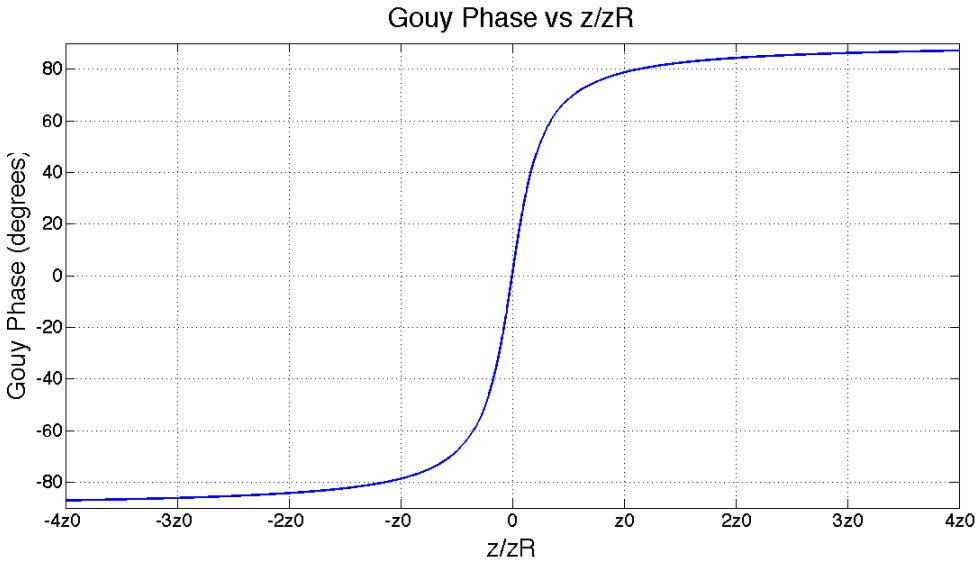

Figure 2: The Gouy phase as function of z. As the gaussian beam propagates from $-\infty < z < +\infty$, the Gouy phase approaches to $\pm\frac{\pi}{2}$

2.2 Vector Phase of the Optical System and the use of Gouy Phase Separation

The laser field of a propagating gaussian beam in an optical system can be represented in a vector space in which optical elements such as mirrors are treated as operators in the vector space[6]. By using this vector space representation, we can represent the alignment of

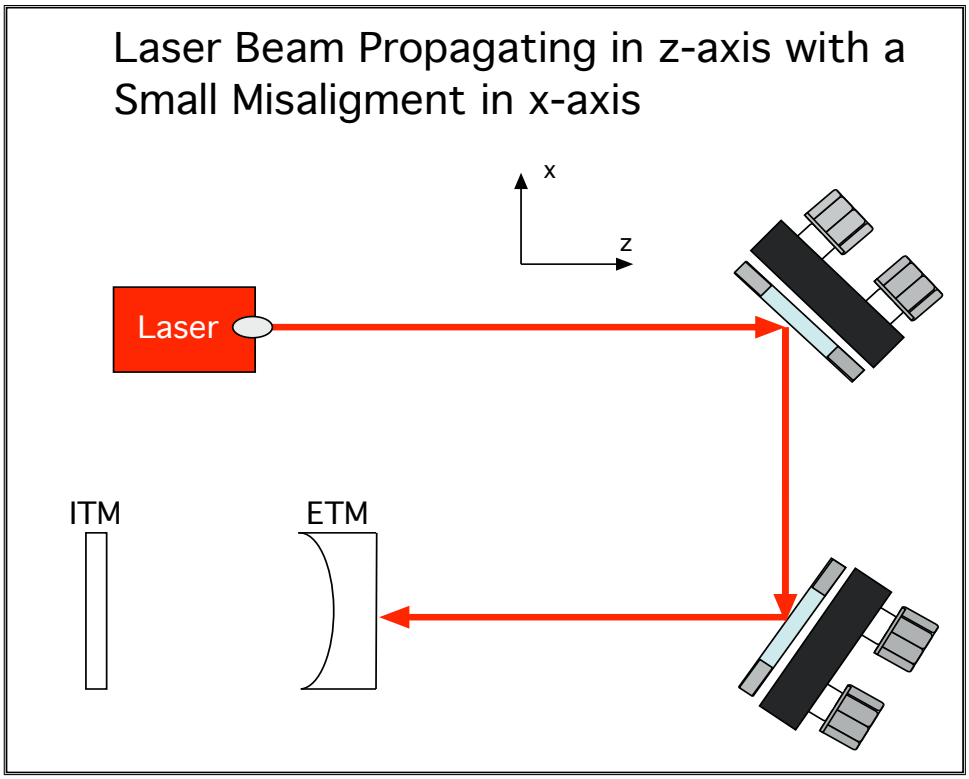

Figure 4: Optical system in which there is a small misalignment in the x direction

the laser beam going into a cavity. The alignment of the laser beam into the cavity will have four degrees of freedom namely beam waist position and beam waist angle in the x and y direction[6]. The mirrors that are used for actuating on the laser beam can be represented as vectors in this vector space. In a good alignment system, ideally we would like to have a mirror that is close to near field of the gaussian beam and another mirror that is in the far field of the gaussian beam. By having a system like this, it would ensure that actuating on one mirror would mostly control the angle of the beam while actuating on the second mirror would mostly control the displacement of the beam. In other words, in an ideal alignment system, we would like to have a Gouy phase separation between two mirrors to be close to 90^o. Let's take a look at why this is the case.

Let's imagine that we are in a single plane of beam alignment where we are only concern with the waist position and the angle in the x direction, and there is a small misalignment in x as shown in Figure 4. As we saw previously, misalignment can be represent as a superposition of the TEM_{00} and TEM_{10} in which would have the following expression:

$$|E\rangle = TEM_{00} + \left(\frac{\delta x}{w_o} + i\frac{\theta}{\theta_d}\right) TEM_{01} \tag{7}$$

where δx is the beam position displacement, θ is the tilt angle, and θ_d divergence angle, which is given by $\theta_d = \frac{\lambda}{(\pi w_0)}$ [6]. In this Equation 7, we can see that how well we can control the beam position and displacement will depend on our ability to control the real and imaginary of the TEM_{10}. By controlling the imaginary and the real component of the TEM_{10} independently, this will yield the a good alignment system.

Now, if we take our alignment system in Figure 4, we can represent the first mirror and the second mirror as A and B respectively, and write the vector operator for each mirror and get the following[6]:

$$M_A = \begin{bmatrix} 1 & -2i\theta_A \\ -2i\theta_A & 1 \end{bmatrix} \tag{8}$$

$$M_B = \begin{bmatrix} 1 & -2i\theta_B \\ -2i\theta_B & 1 \end{bmatrix} \tag{9}$$

where θ_A and θ_B are alignment angle of mirrors A and B respectively. Since the two mirrors are separated by a distance, we can write an operator for the propagation phase in which the TEM_{10} mode experience an additional Gouy phase φ. This propagation operator is given by[6]:

$$P = e^{i\phi} \begin{bmatrix} 1 & 0 \\ 0 & e^{i\varphi} \end{bmatrix} \tag{10}$$

Let's apply the operators to a pure TEM_{00} input field ignoring the overall phase. We will get the following:

$$M_B P M_A = \begin{bmatrix} 1 & -2i\left(\theta_A + e^{i\varphi}\theta_B\right) \\ -2i\left(e^{i\varphi}\theta_A + \theta_B\right) & e^{i\varphi} \end{bmatrix} \tag{11}$$

$$|E\rangle_{out} = TEM_{00} - \left(e^{i\varphi}\theta_A + \theta_B\right) TEM_{01} \tag{12}$$

Now, if we take a look at Equation 7 and we compare it with Equation 12, we notice that θ_B exclusively actuate on the angle, while θ_A would only actuate on the displacement of the beam if the Gouy phase separation between the two mirrors is 90^o. In other words, this illustrates that the Gouy phase separation between the two mirrors will determine the orthogonality of the actuators. This means if the Gouy phase separation is 90^o as shown in Equation 12, we would have orthogonal actuators. Having orthogonal actuators then would give us a good alignment system control.

3 X-arm Auxiliary Laser Current Alignment Issues and Its Solution

3.1 Current X-arm Green PZT Steering Mirrors Issues

The x-arm auxiliary laser is used for locking the x-arm cavity. In order to lock the cavity to the 1064nm interferometer pre-stabilized IR Laser (PSL), it is necessary to lock the auxiliary laser frequency to the cavity. The auxiliary laser beam goes through a single path Second Harmonic Generator (SHG) where the auxiliary laser is converted into green light. The green light is sent into the cavity by using two PZT mirrors. The PTZ mirrors are actuating until the green light is aligned in the cavity and therefore resonance is achieved. When the light resonate inside the cavity, it gets transmitted through the ITM. Then, using the Pound-Drever Hall technique and other techniques, which I will not mention in this paper, an error

signal is obtained. This signal is used for controlling the cavity and therefore locking it. As we can see, it is essential to have a good alignment system for the auxiliary laser.

The current issues with the x-arm auxiliary laser is that the two PZT mirrors that actuate on the beam are too close to each other as shown in Figure 5. This is a problem because when actuating on both mirrors, we get that both of them are acting as if there were just a single mirror, producing a small change on both angle and position. In other words, the Gouy phase separation between the two PZT mirrors is not 90^o. As we saw in previous section, this is not a good alignment system because when we align the system, we don't have full control of the degrees of freedom, and therefore it is more troubling to align the system.

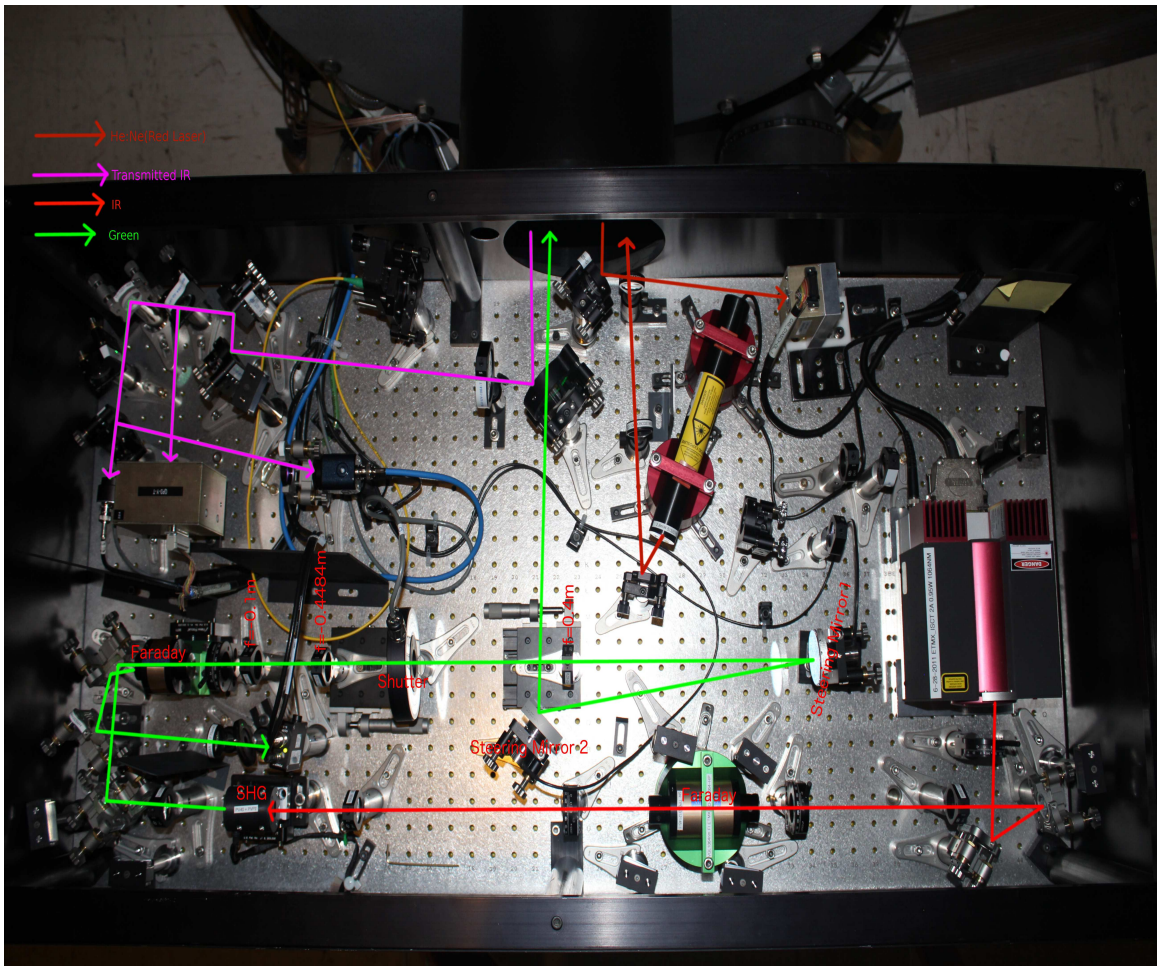

Figure 5: Xarm Original Optical Table Setup

3.2 Designing a New Optical Table Setup

Before we proceeded to design a new optical setup for this system, we need to calculate the Gouy phase separation between the two PZT mirrors and the mode matching of the cavity. In Figure 5, we know that at the SHG the waist of the gaussian beam is 35.36μm, and by measuring and calculating the optical path length between each components relative to the

SHG we can calculate the Gouy phase separation and the mode matching. Using a la mode, a matlab program, we found that the current mode matching is 0.9343 and that the Gouy phase separation between the PZT mirrors is 0.2023^o. In order to verify the mode matching value that we obtained from the calculation, we locked the x-arm to the PSL, and we scan the transmitted green light as shown in Figure 6. We calculated the mode mismatch, which is given by the ratio of the small circle peak over the high circle peak. The equation for the mode matching is given by mode matching $= 1 -$ mode mismatching. Therefore, we found that the mode matching is 0.9215, which is close to the calculated mode matching.

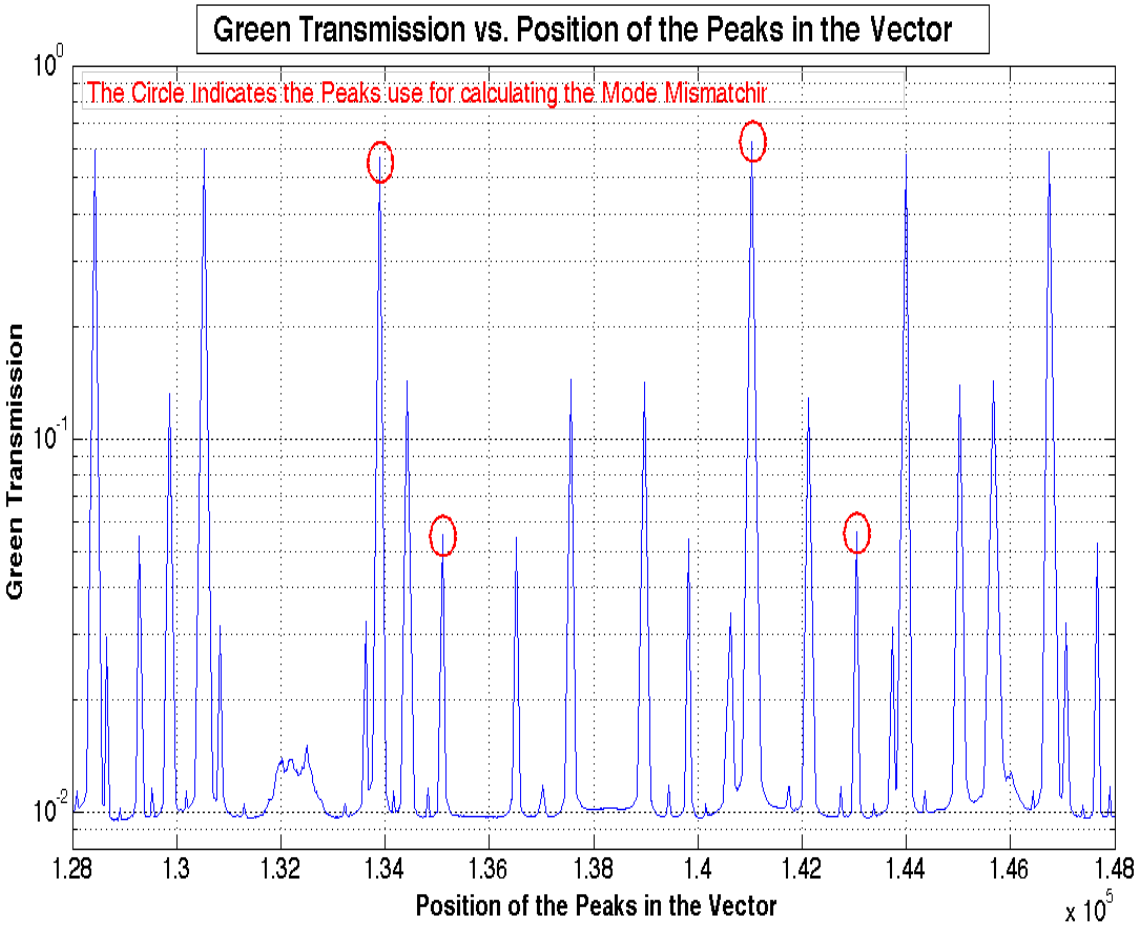

Figure 6: Measurement of Mode Matching. The two highest circled peaks are the TEM00 mode. The two other circled peaks are the higher order TEM modes.

After obtaining the current mode matching and the current Gouy phase separation between the steering mirrors, we try to increase the Gouy phase by using more lenses and leaving the two PZT mirrors where they are. However, we realized that it was not possible to increase the Gouy phase separation without sacrificing the mode matching. Therefore, we had to come up with a new solution that involves increasing the optical path by adding two more mirrors as shown in Figure 7. Figure 7 illustrates the new possible setup that we came up with. By looking at Figure 5, we approximated the possible places where new mirrors and new lenses should be placed.

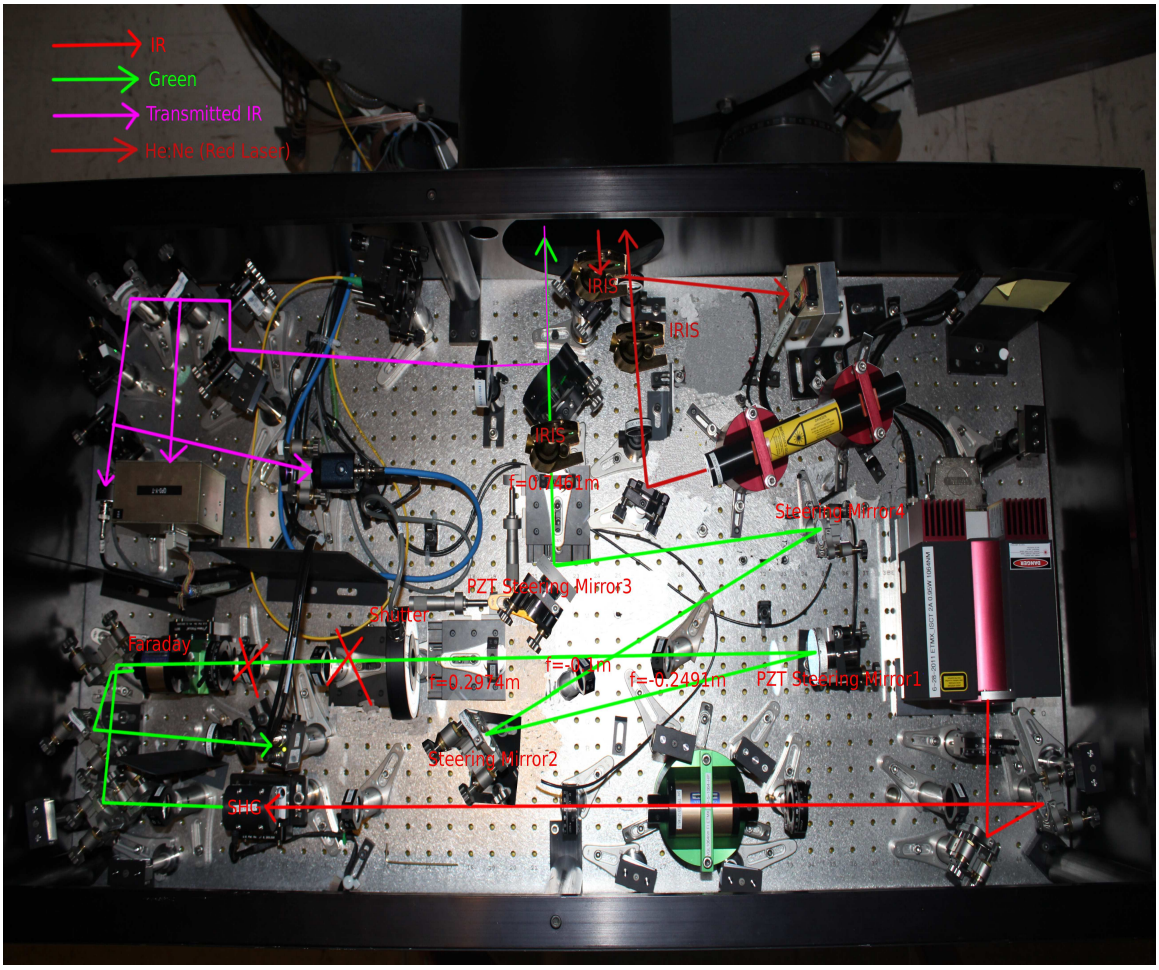

Figure 7: 40m New Upgrade Xarm Predicted Optical Table Setup

Then, using a la mode, we parameterize the displacement of the lenses and mirror, and we optimize the solution. The following table is the results obtained:

label	z (m)	type	parameters (m)
Lens 1	0.0800	Lens	Focal Length: 0.100
First Mirror	0.1550	Flat Mirror	none
Second Mirror	0.2800	Flat Mirror	none
Lens 3	0.6542	Lens	Focal Mirror: 0.2974
Lens 4	0.8914	Lens	Focal Mirror: -0.249
Third Mirror	1.0675	Flat Mirror	none
Fourth Mirror	1.4183	Flat Mirror	none
Lens 5	1.5338	Lens	Focal Mirror: -0.100
Fifth Mirror	1.7836	Flat Mirror	none
Sixth Mirror	2.1344	Flat Mirror	none
Lens 6	2.2106	Lens	Focal Length:0.7461
ETMX	2.7892	Lens	Focal Length:0.2974
ITMX	40.5792	Flat Mirror	none

The new optical table setup give us a mode matching of 0.99144 and a Gouy phase separation

of 85.23° between the third steering mirror and sixth steering mirror as shown in Figure 8.

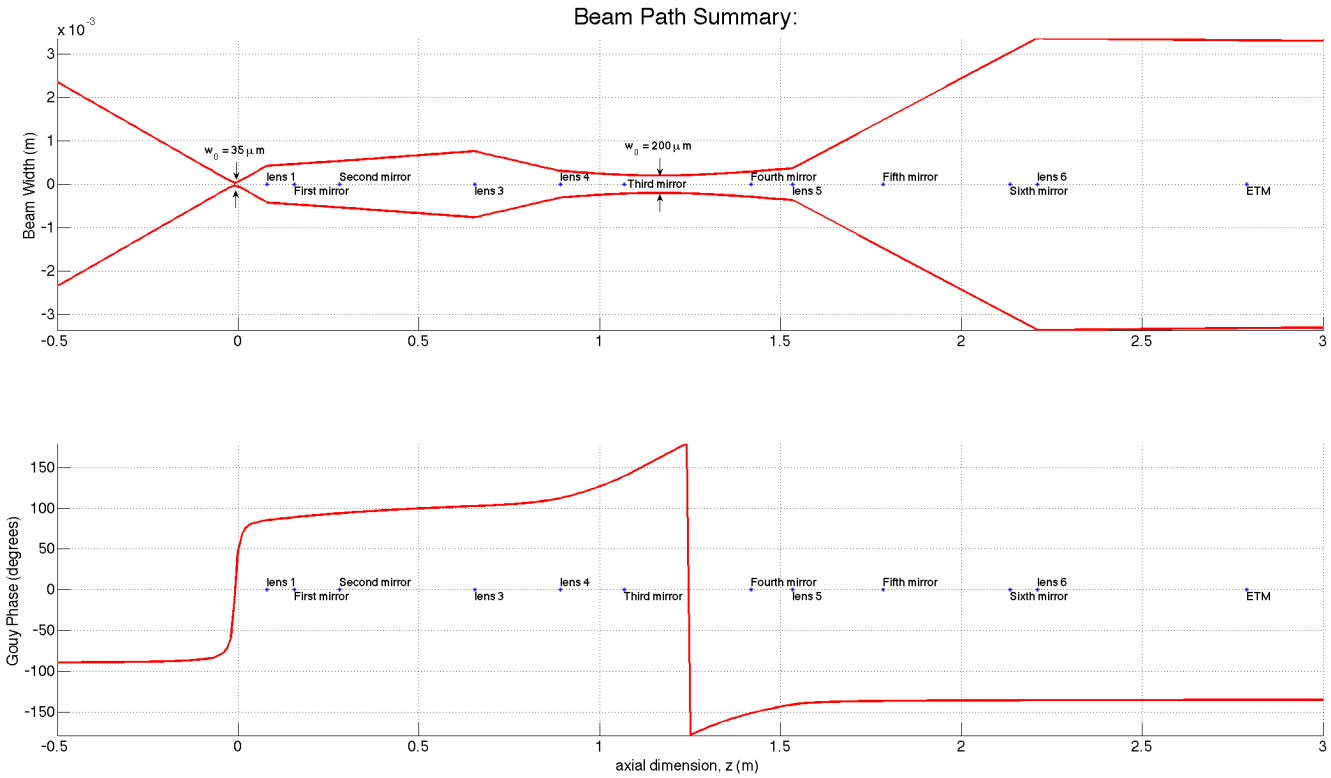

Figure 8: A la Mode Results for the Position of the Lenses

In order to be able to see how much improvement the new setup provides us over the current setup, we plotted the $\Delta y/v$ versus $\Delta\theta/v$ as shown in Figure 9. In Figure 9, the dotted lines show the original optical setup, and as we can see the two vectors are closed to each other, which is telling us that moving either or both mirrors results in small angle change and beam translation. This illustrates that both of the mirrors in the current optical setup are acting as if they were just a single mirror. However, in the new setup, we can see that one of the mirror give mostly angle changes while the other mirror give us mostly beam translation, which implies a good Gouy phase.

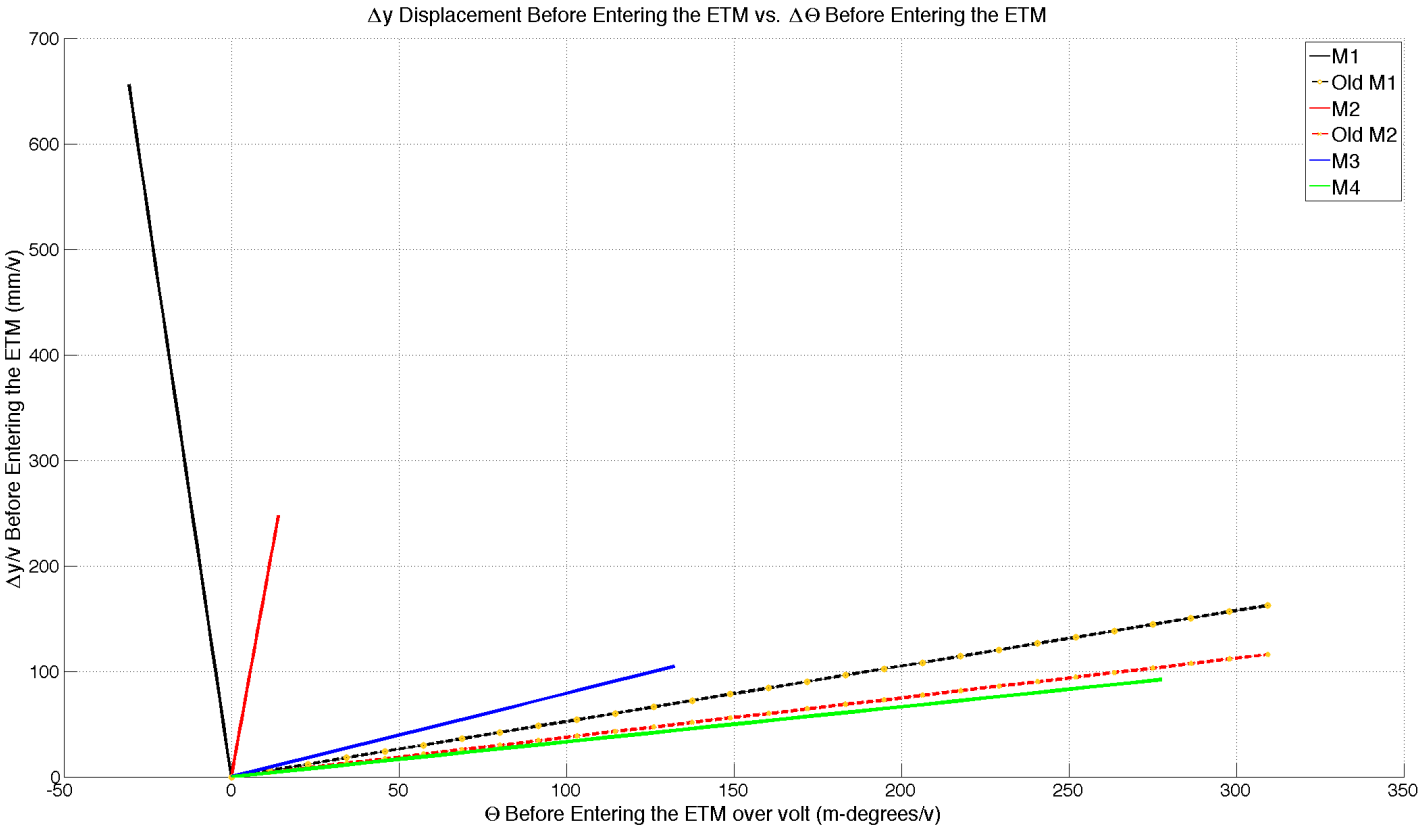

Figure 9: By changing the angles of the mirrors, we obtain a change in the beam translation at the ETM. $\Delta y/v$ as a function of θ/v at the ETM. The dotted lines correspond to the current optical setup, and the solid lines are the new optical setup.

After finishing all the calculation for the new optical setup, we proceeded with the upgrade. Before we started to remove the original optical elements in the table, we positioned two irises, one before the harmonic separator and the other before the He:Neon red laser so that we can maintain the same optical axis as the current setup. All the optical components in the table above were placed in their corresponding position. The new optical setup is shown in Figure 10. Even though we did not characterize the new optical setup, everything seems to be working much better than how it was working before.

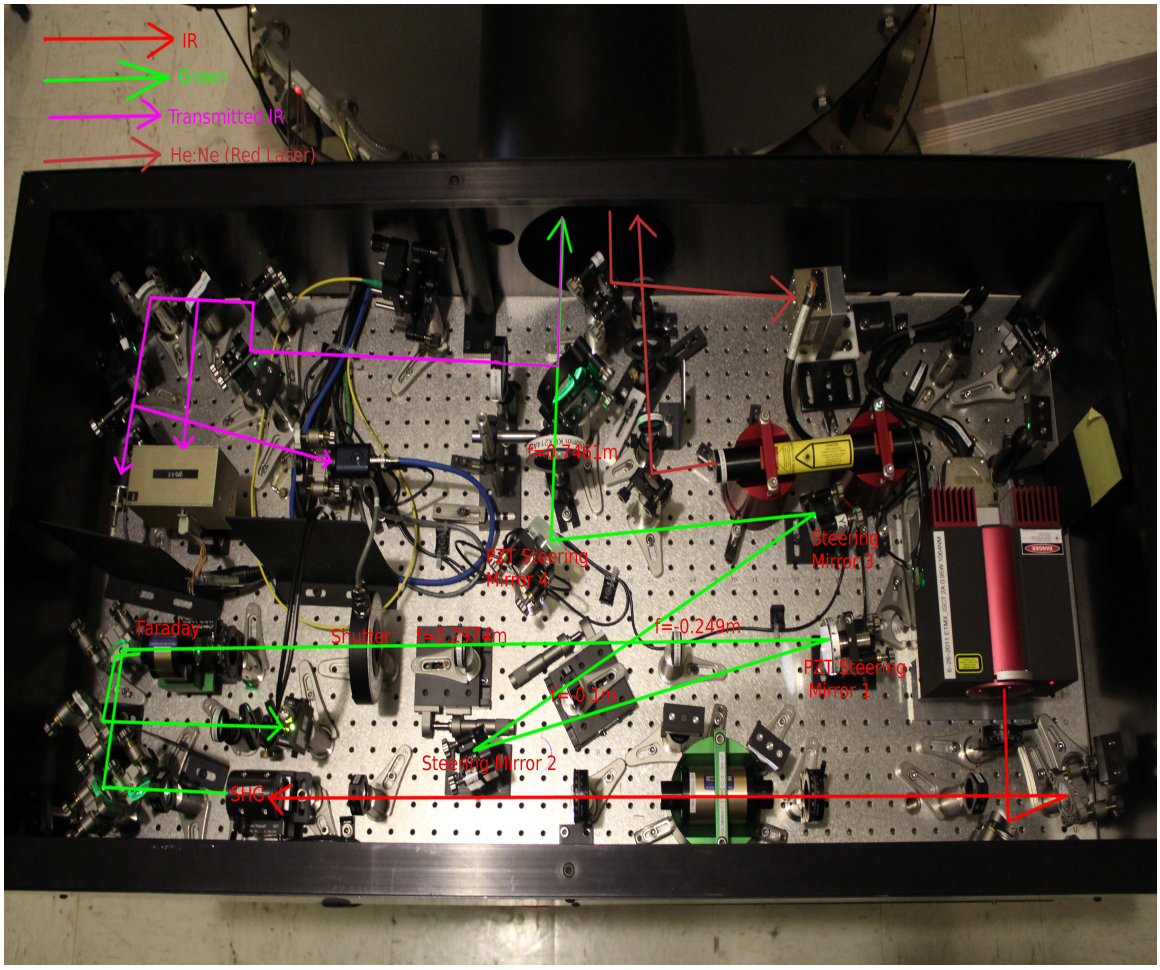

Figure 10: 40m New Upgrade Xarm Optical Table Setup

4 Input Mode Cleaner Current Issues and Its Solution

The function of the input mode cleaner is to suppress higher-order TEM modes and to filter laser amplitude and frequency fluctuations[3]. The input mode cleaner used in the 40 meter prototype interferometer is a ring cavity that consists on three mirrors: two suspended flat mirrors and one suspended curve mirror as showing in Figure 11.

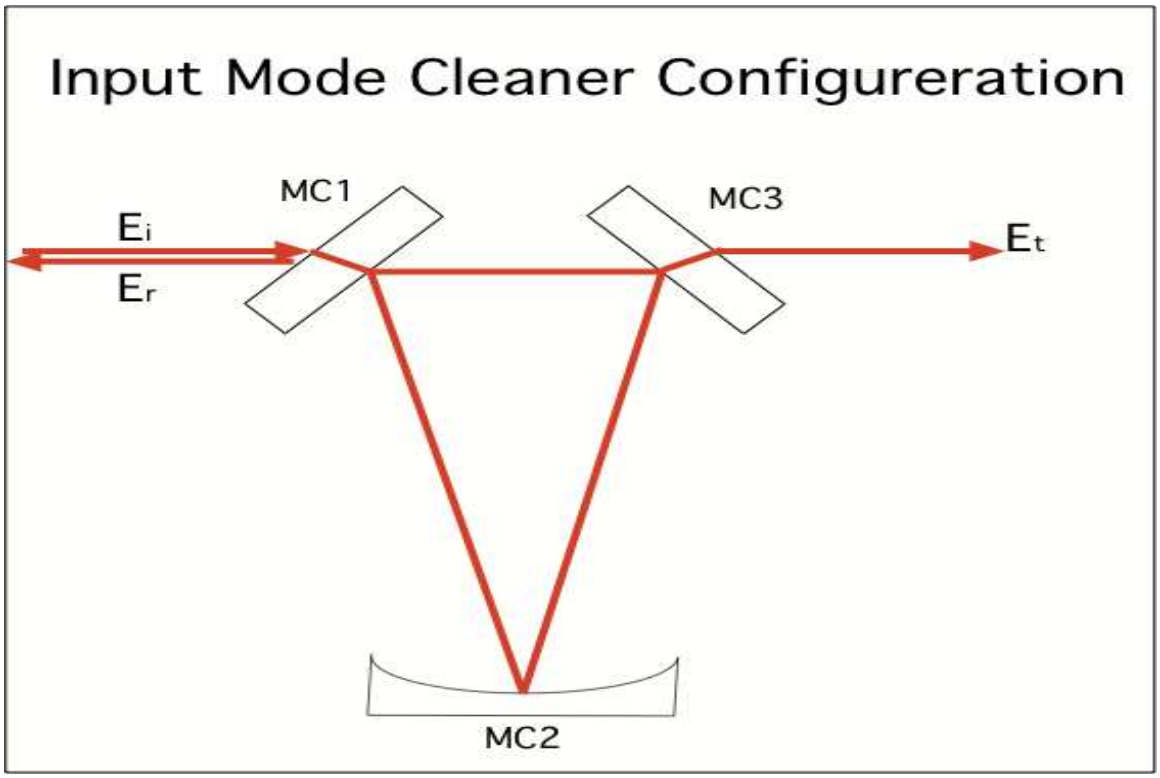

Figure 11: Input Mode Cleaner Schematic

Due to the fact that any higher order TEM modes inside the Fabry-Perot cavity arms can compromise the signal to noise ratio, we need to make sure that the input mode cleaner is well align at all times. In order to obtain a good alignment system for the input mode cleaner, two wavefront sensors are used for detecting misalignment. We would see that the concept of having a Gouy phase separation of 90^o between wavefront sensors is important for detecting misalignment associate with the mirrors. By having a Gouy phase separation of 90^o, this means that one of the wavefront sensors would be able to detect angle misalignment while the other wavefront sensor would be able to detect beam displacement misalignment.

The current issues of the input mode cleaner wavefront sensors is that the Gouy phase separation between the two wavefront sensors is not 90^o. Figure 12 illustrates the original optical table setup for the input mode cleaner wavefront sensors. Before we tried to design a new optical setup, we needed to calculate the current Gouy phase separation between the two wavefront sensors. Since we were not able to measure the waist size of the beam in order to used it in a la mode, we instead measured the distance that the first lens is away from the MC1 (first mirror). Then, since we knew the relative distance between MC1, MC2, and MC3, we mode matched the beam to the cavity, and we propagated it backward. For the original setup, we calculated the Gouy phase separation between the wavefront sensors to be 49.675^o. After knowing that, we designed a new optical table setup in which each wavefront sensor would be placed facing west and the waist size at the wavefront sensors would be within the range of 1mm to 2mm.

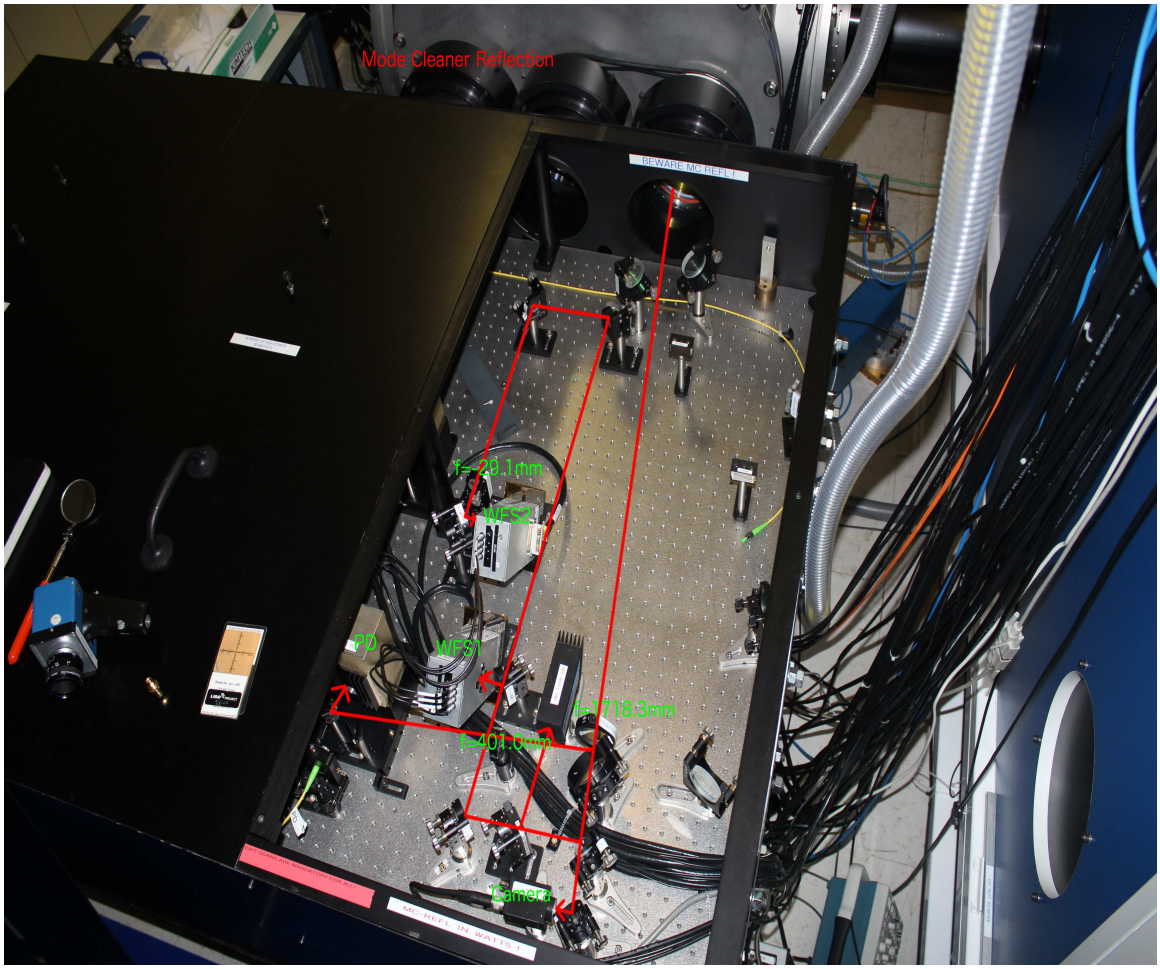

Figure 12: Original Optical Table Wavefront Sensor Setup for the Input Mode Cleaner

We designed a new possible optical table setup in which we placed the wavefront sensors facing west as shown in Figure 13. Then, we estimate the position where each optical elements should be placed, and we used a la mode. Since in a la mode the optical components of a system is placed in one dimension, we had to create two beam paths in order to simulate the design that would satisfy the boundary condition: a waist size at the wavefront sensors ranging between 1mm to 2mm and sensors placed facing west. For the beam of the first wavefront sensor, we obtained the results in Table 1. We did the same for the wavefront sensor two, and we found the results in Table 2 . We found that the Gouy phase separation between the wavefront sensor is 89.37^o. Figure 14 and Figure 15 show he beam profile for the wavefront sensor one and two respectively in which can be observed that the waist size at the wavefront sensor one and two is about 1mm.

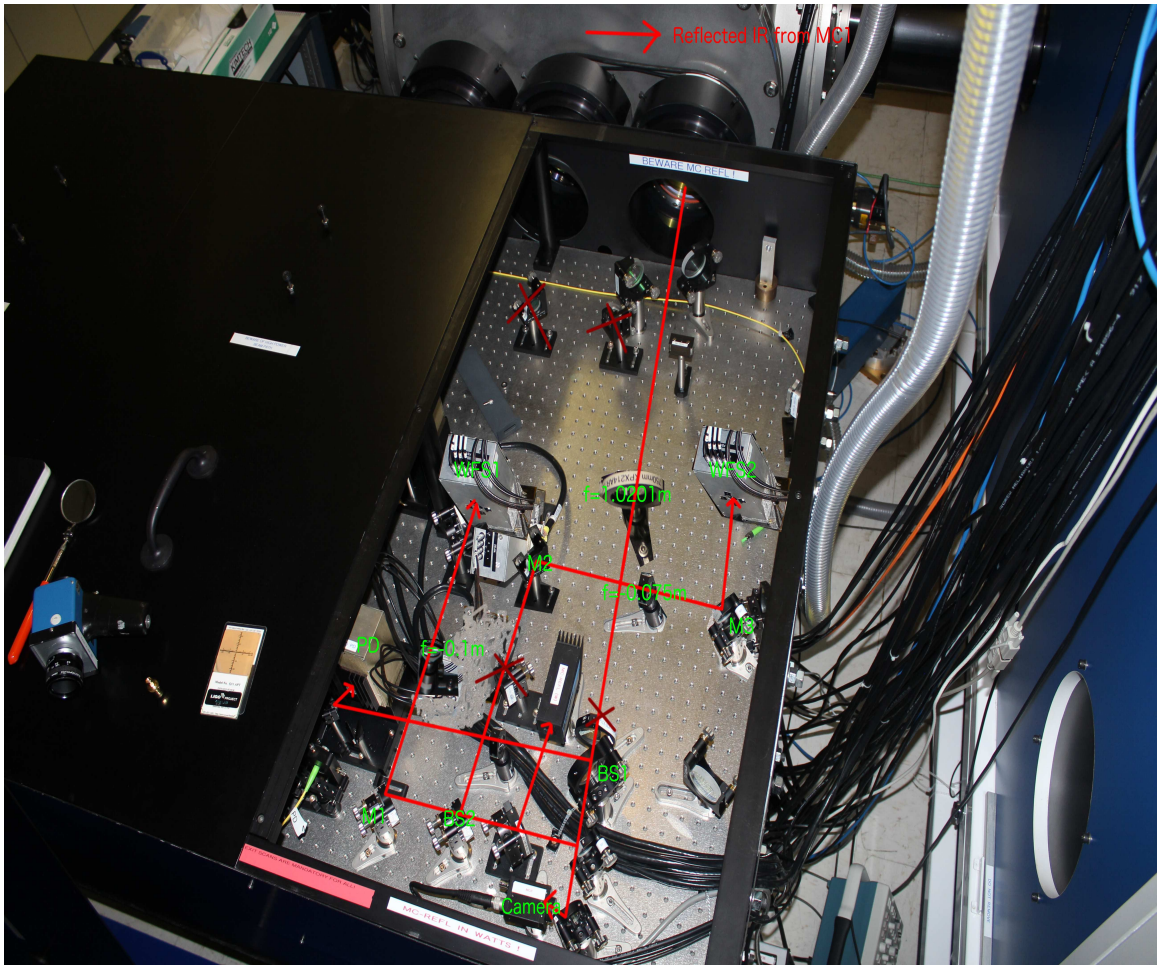

Figure 13: The new design for the input mode cleaner wavefront sensor

label	z (m)	type	parameters (m)
MC1	0	Flat Mirror	none
MC3	0.1753	Flat Mirror	none
MC2	13.4587	Curved Mirror	ROC: 17.870
Lens 1	29.3705	Lens	FocalLength: 1.0201
BS2	29.9475	Beam Splitter	none
First Mirror	30.0237	Flat Mirror	none
Lens2	30.2000	Lens	Focal Length: -0.100
WFS1	30.4809	WaveFront Sensor 1	none

Table 1: Beam Path for the Wavefront Sensor 1

label	z (m)	type	parameters (m)
MC1	0	Flat Mirror	none
MC3	0.1753	Flat Mirror	none
MC2	13.4587	Curved Mirror	ROC: 17.870
Lens 1	29.3705	Lens	FocalLength: 1.0201
BS2	29.9475	Beam Splitter	none
Second Mirror	30.2650	Flat Mirror	none
Lens3	30.4809	Lens	Focal Length: -0.075
Third Mirror	30.5698	Flat Mirror	none
WFS2	30.6968	WaveFront Sensor 2	none

Table 2: Beam Path for the Wavefront Sensor 2

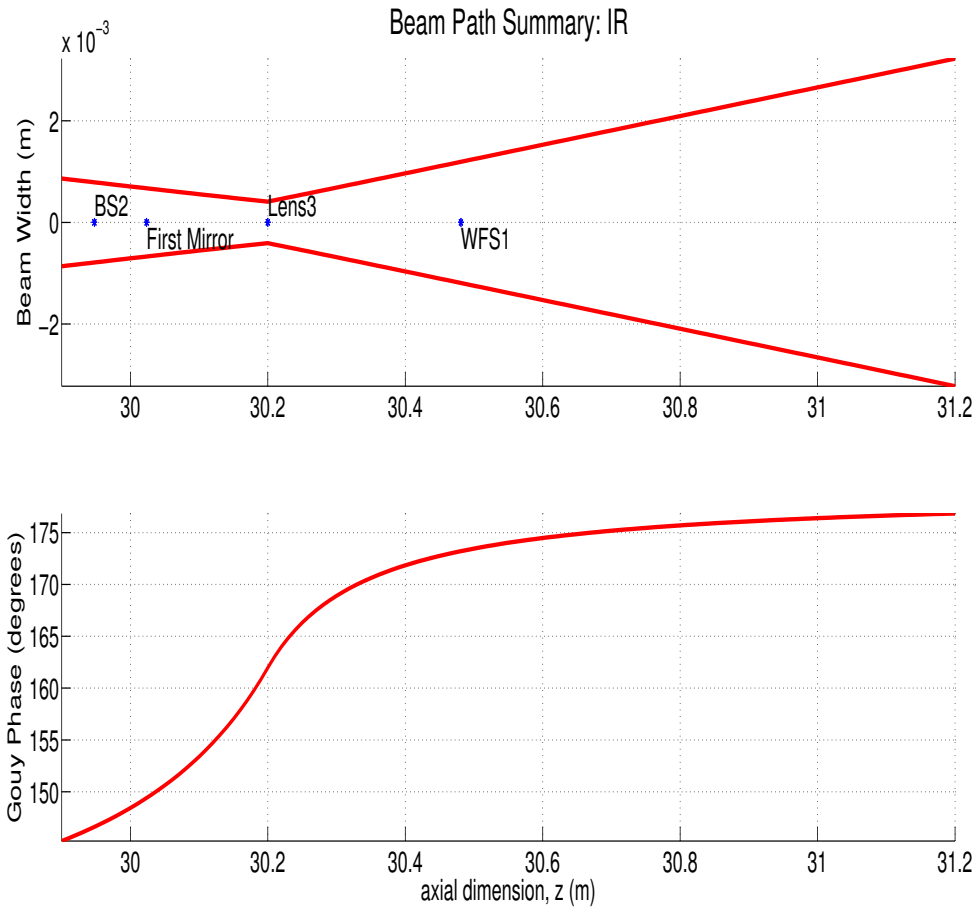

Figure 14: A la mode Beam Plot for the Wavefront Sensor 1

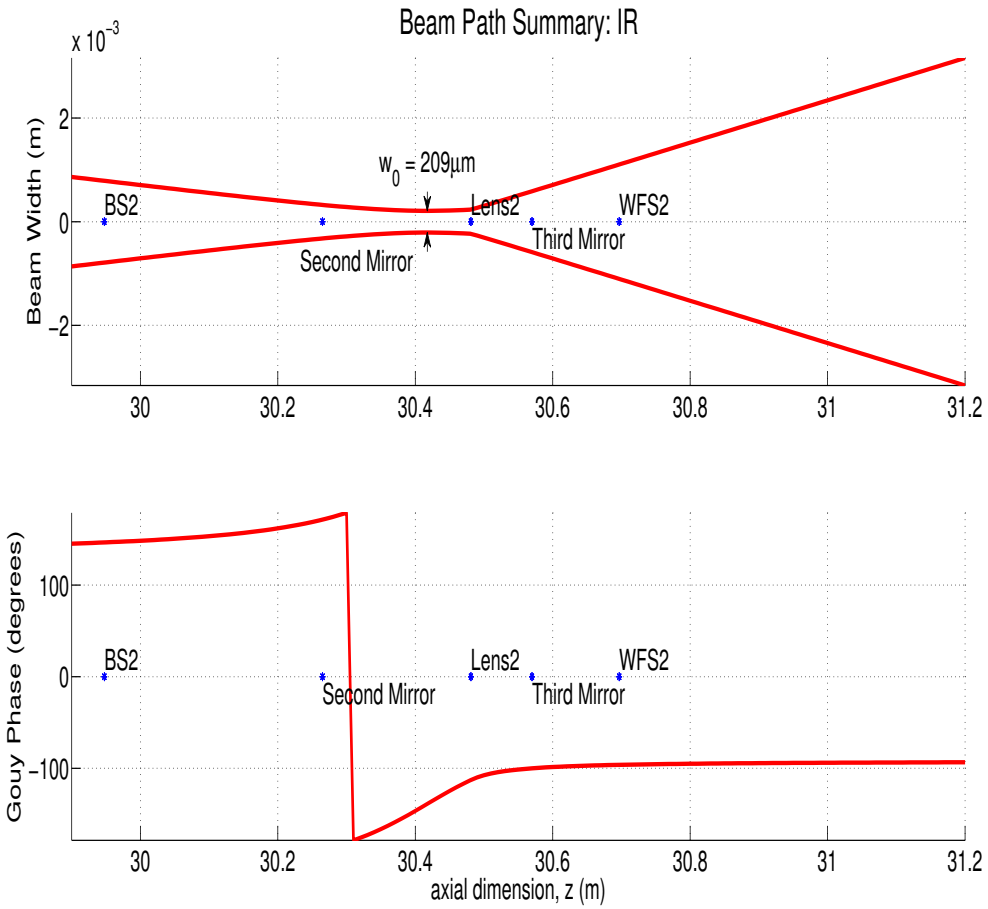

Figure 15: A la mode Beam Plot for the Wavefront Sensor 2

Based on the design in Figure 13, we placed the optical components where they should be placed. While positioning the optical components, we centered the beam on the of the optical elements, and aligned the beam into the wavefront sensors as well. The new design of the optical table for the wavefront sensors is shown if Figure 16. Unfortunately, we could not do an analysis on the performance of the Wavefront sensors after the upgrade, but that will be done in the future.

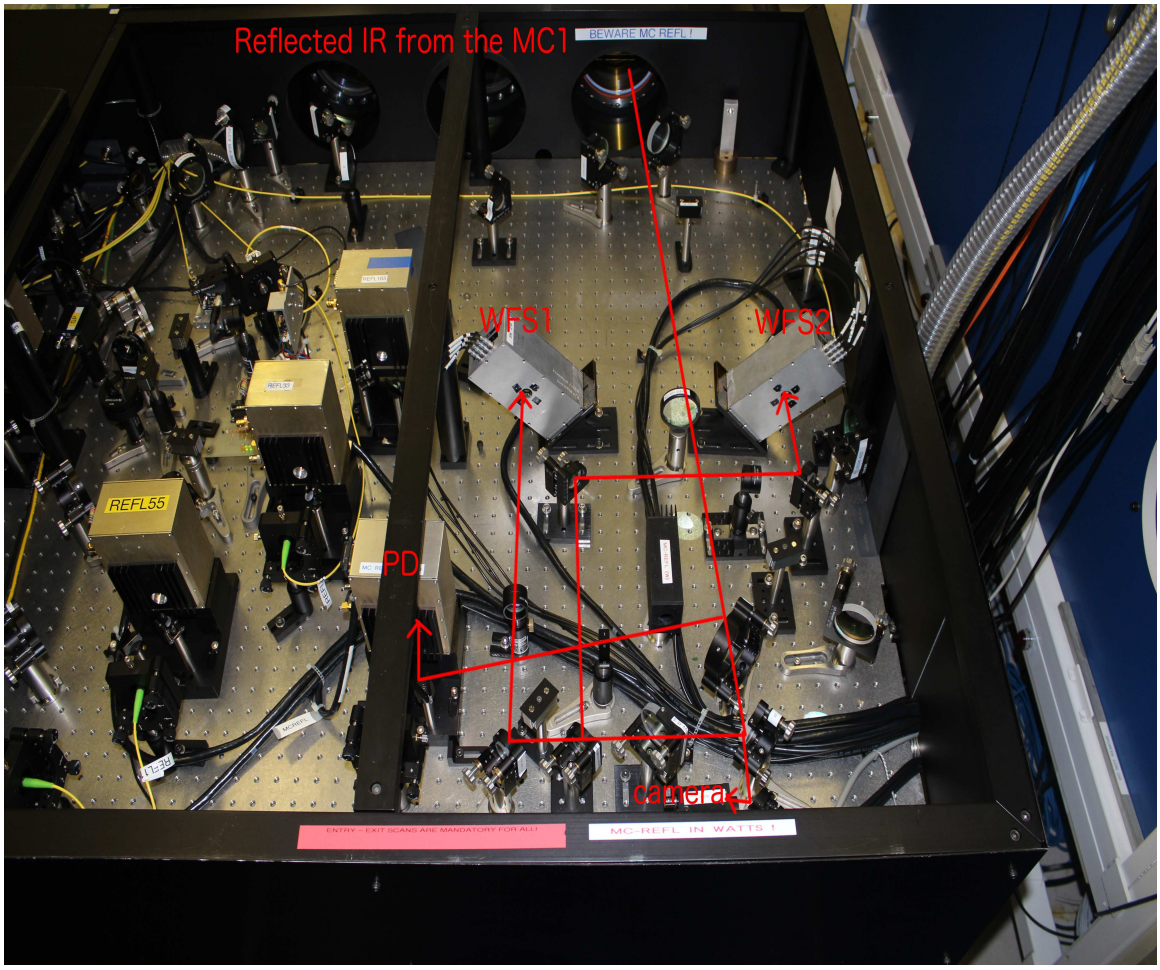

Figure 16: The actual new optical table setup for the input mode cleaner wavefront sensors after the upgrade was done.

5 Conclusion

In this paper, we designed an optical setup for the x-arm green PTZ steering. In this new optical table setup, we were able to increase the Gouy phase separation from 0.2023^o to 85.23^o, which is better than what it was before. For the input mode cleaner wavefront sensors, we designed a new optical setup that increases the Gouy phase separation from 49.675^o to 89.37^o, which give us more control of the degrees of freedom. Even though we were not able to characterize the improvement of the new alignment optical system, the system seems to be better than what is was before the upgrade. For future work, we need to characterize both the Gouy phase separation of the x-arm green steering mirrors, and the input mode cleaner wavefront sensors.

References

[1] McClelland, D.E., Mavalvala N., Chen Y., &Schnabel R., *Advanced interferometry, quantum optics and optomechanics in gravitational wave detectors*. Laser & Photonics Reviews, 5.5 (2011):677-696.

[2] Schnabel, R., Mavalvala N., McClelland, D.E., & et. al, *Quantum metrology for gravitational wave astronomy*. Nature Communications, 1 (2010):121.

[3] Grote, H., Heinzel, G., Freise, A., & Lam P.K., *Automatic beam alignment for the mode-cleaner cavities of GEO 600*, Applied Optics, 43.9 (2004):1938-1945.

[4] Saleh, B.E., & Teich, M.C., *Fundamentals of Photonics*, Canada, Wiley Interscience (1991): 3.

[5] Siegman, A.E., *Lasers*, Sausalito, CA: U Science (1986).

[6] Smith-Lefebvre, N.M., *Techniques for Improving the Readout Sensitivity of Gravitational Wave Antennae*, http://www.ligo.mit.edu/ nsmith/nicolas-thesis.pdf.

[7] Wikipedia, *Gaussian Beam*, Wikipimedia Foundation, http://upload.wikimedia.org/wikipedia/commons/b/be/Hermite-gaussian.png

[8] Izumi, K., Arai, K., Barr, B., & et al., *Multicolor cavity metrology*, JOSA A 29.10 (2012): 2092-2103.

[9] Anderson, D.Z., *Alignment of resonant optical cavities*, Applied Optics 23.17 (1984): 2944-2949.